

# Glucose transport and apoptosis after gene therapy with HSV thymidine kinase

Uwe Haberkorn<sup>1, 3</sup>, Annette Altmann<sup>3</sup>, Huse Kamencic<sup>2</sup>, Iris Morr<sup>3</sup>, Ulrike Traut<sup>2</sup>, Marcus Henze<sup>1, 3</sup>, Shiming Jiang<sup>3</sup>, Jürgen Metz<sup>2</sup>, Ralf Kinscherf<sup>2</sup>

<sup>1</sup> Department of Nuclear Medicine, University of Heidelberg, Im Neuenheimer Feld 400, 69120 Heidelberg, Germany

<sup>2</sup> Department of Anatomy and Cell Biology III, University of Heidelberg, Germany

<sup>3</sup> Clinical Cooperation Unit Nuclear Medicine, German Cancer Research Center, Heidelberg, Germany

Received 10 April and in revised form 16 August 2001 / Published online: 19 September 2001

© Springer-Verlag 2001

**Abstract.** The relation between tumour metabolism and induction of apoptosis by gene therapy was investigated in a rat Morris hepatoma (MH3924A) model expressing the HSV thymidine kinase (*HSVtk*) gene. In vivo the amount of glucose transporter (GLUT1 and GLUT3 isoforms) expressing cells was determined in tumours of untreated and treated animals using immunohistochemistry. In vitro uptake studies with 2-fluoro-2-deoxy-D-glucose (FDG), 3-*O*-methylglucose and thymidine (TdR) and a TUNEL (TdT-mediated dUTP nick end labelling) assay for the assessment of apoptosis were done immediately and 24 h after treatment of the recombinant cells with different doses of ganciclovir (GCV). Immunohistochemistry revealed a significant increase in GLUT1 in treated tumours which showed enhanced transport activity for FDG. In vitro the FDG and 3-*O*-methylglucose uptake increased to 186% when compared with that of the non-treated cells immediately after incubation with GCV. However, 24 h later the FDG uptake had declined to its normal level, whereas the accumulation of 3-*O*-methylglucose remained elevated. The uptake of TdR, which was determined simultaneously, decreased in the acid-insoluble fraction of the cells to 27% and 11%, respectively, immediately and 24 h after therapy, while in the acid-soluble fraction it increased to 229% and to 167%, respectively. Employing the TUNEL technique, 25% of cells were found to be apoptotic 24 h after the termination of GCV treatment. Inhibition of glucose transport by cytochalasin B or competition with deoxyglucose resulted in a 78% (cytochalasin B) and 88% (deoxyglucose) decrease in FDG uptake in the recombinant hepatoma cells and in an increase in the apoptotic cell fraction. It is concluded that inhibition of enhanced glu-

cose transport in GCV-treated cells increased apoptosis. Therefore, enhanced glucose transport seems to represent a stress reaction of tumour cells dedicated for the prevention of cell death.

**Keywords:** Gene therapy – HSV thymidine kinase – Apoptosis

**Eur J Nucl Med (2001) 28:1690–1696**

DOI 10.1007/s002590100644

## Introduction

Gene therapy based on the transduction of the herpes simplex virus thymidine kinase (*HSVtk*) gene and ganciclovir (GCV) treatment has been shown to be effective in a variety of malignant tumour models in vitro and in vivo [1, 2, 3, 4, 5, 6]. GCV and other nucleoside analogues are converted by the *HSVtk* to their monophosphate metabolites, which are subsequently phosphorylated by cellular kinases to di- and triphosphates [7]. After insertion of GCV metabolites into the cellular DNA during replication, chain termination originates followed by cell death. Furthermore, non-transduced tumour cells in close proximity to *HSVtk*-expressing cells become sensitive to GCV treatment (“bystander effect”). Apoptosis has been proposed as a mechanism by which killing of transformed cells and also of bystander cells is mediated [8, 9, 10, 11]. Hamel et al. found that apoptosis in bystander cells during GCV therapy involves a pathway that can be inhibited by the proto-oncogene *Bcl-2* [9]. Employing the human neuroblastoma cell line SH-EP for detailed molecular analysis, strong expression and aggregation of the APO-1/CD95/Fas receptor and up-regulation of *p53*, both molecules involved in the induction of apoptosis, were shown to be induced in these cells upon *HSVtk*/GCV gene therapy [12]. Additional evidence for

Uwe Haberkorn (✉)

Department of Nuclear Medicine, University of Heidelberg,

Im Neuenheimer Feld 400, 69120 Heidelberg, Germany

e-mail: Uwe\_Haberkorn@med.uni-heidelberg.de

Tel.: +49-6221-567731

the concept of death-receptor mediated apoptosis was derived from observations that in the presence of a caspase inhibitor, the apoptotic cell fraction decreased, and that GCV-treated cells were sensitive to the tumour necrosis factor receptor-1 and TRAIL receptor-induced apoptosis [12].

Apoptosis and necrosis are often observed simultaneously in tissues or cell cultures exposed to the same stimulus. Therefore, a downstream control mechanism has been postulated which directs cells towards necrosis or apoptosis. Since apoptosis is known to be an energy-consuming process, studies of the tumour metabolism early after treatment are of interest for the biochemical characterisation of the tumour's response to gene therapy [13, 14, 15]. In previous studies using positron emission tomography (PET) we found evidence for an uncoupling of glucose transport and phosphorylation in *HSVtk*-expressing tumours early after treatment with GCV as a reaction of the tumour cells to cellular stress [16, 17]. Since the *HSVtk* suicide system interferes with DNA synthesis, this process may be similar to that which occurs when using conventional cancer treatments applying chemotherapeutic drugs or radiation, which may result in apoptosis. Therefore, the present study was done to investigate the relation of metabolic changes to the process of programmed cell death.

## Materials and methods

**Immunohistochemistry in animal tumours after gene therapy.** An animal study was performed using LXSNTk8, an *HSVtk*-expressing cell line derived from the Morris hepatoma cell line MH3924A [17, 18]. Four  $\times 10^6$  tumour cells were transplanted subcutaneously into the right thigh of male young adult ACI rats. At 21–28 days after inoculation, when the tumours had reached a diameter of more than 20 mm, the animals (weighing 260–393 g) were treated by daily intraperitoneal administration of 100 mg GCV/kg body weight for 2 days. A control group received sodium chloride for 2 days.

The animals first underwent a PET examination of the 2-fluoro-2-deoxy-D-glucose (FDG) transport and phosphorylation [17]. Immediately after the PET examination, the animals were sacrificed, the tumours were rapidly removed and specimens were snap-frozen in liquid nitrogen-cooled isopentane for immunohistochemistry. Immunohistological and morphometric analyses were performed in five control animals and in five animals 2 days after initiation of GCV treatment with elevated FDG transport as shown by PET [17]. Immunohistochemistry was routinely performed as previously described [19, 20]. In detail, 6- $\mu$ m sections were cut on a cryostat, placed on silan-precoated slides, fixed with acetone ( $-20^\circ\text{C}$ , 10 min) and dried (10 min). Non-specific sites were blocked with 1% normal swine serum (Life Technologies) in phosphate-buffered saline (PBS; 10 min). For immunostaining of the cryosections, polyclonal rabbit anti-rat GLUT1 and anti-rat GLUT3 (each 1:1000 in PBS,  $37^\circ\text{C}$ , 90 min; both from Chemicon International, Hofheim, Germany) were used. Endogenous peroxidase was suppressed with 3%  $\text{H}_2\text{O}_2$  in PBS (5 min). Then, sections were incubated with biotinylated anti-rabbit immunoglobulin and streptavidin-peroxidase (1:100; both from Amersham, Braun-

schweig, Germany). Staining reaction was performed by adding 3-3'-diaminobenzidine (DAB; Pierce, Rockford, Ill., USA). Finally, nuclei were counterstained with haematoxylin. Rinsing steps with PBS were included. For morphometry, sections were recorded by a three-chip CCD video camera (Sony DXC-750) mounted on a microscope (Olympus BH-2). GLUT1 or GLUT3-immunoreactive cells were marked using a computer-assisted image analysis system (VFG-1 frame grabber; VIBAM software) developed in our group. The percentages of GLUT1- and GLUT3-positive cells were quantified according to procedures previously described [19, 21, 22].

**Cell culture and GCV treatment.** *HSVtk*-expressing rat hepatoma (MH3924Atk8) cells were used for all in vitro experiments [18]. The cells were maintained in culture flasks in RPMI 1640 medium (Gibco BRL, Eggenstein, Germany) supplemented with 292 mg/l glutamine, 100,000 IU/l penicillin, 100 mg/l streptomycin and 20% fetal calf serum at  $37^\circ\text{C}$ , in an atmosphere of 95% air and 5%  $\text{CO}_2$ . The cells were trypsinised, and  $8 \times 10^4$  cells were seeded in six-well plates. Two days later, the cells were treated with 0.5  $\mu\text{M}$ , 5  $\mu\text{M}$  or 25  $\mu\text{M}$  GCV. All uptake experiments were performed immediately and 24 h after the cells had been incubated in the GCV-containing medium. Each of the following experiments was done in triplicate.

**TdR uptake.** The cells were pulsed for 2 h with 185 kBq (*methyl*- $^3\text{H}$ )thymidine (Amersham-Buchler, Braunschweig, Germany; specific radioactivity 185 GBq/mmol; radioactive concentration 37 MBq/ml; radiochemical purity 97.5%) per millilitre of medium and cold thymidine at a final concentration of 0.05 mM. After removal of the medium, the cells were washed three times with ice-cold PBS. The cells were lysed by addition of 0.5 M perchloric acid and removed from the plates with a cell scraper. After 30 min on ice, the cell lysate was vortexed and rotated at  $1,500 \times g$  for 5 min at  $0^\circ\text{C}$ . After the supernatant (acid-soluble fraction) had been removed, the pellet (acid-insoluble fraction) was washed with 0.5 M perchloric acid, centrifuged again for 5 min at  $0^\circ\text{C}$  and resuspended in 1 M NaOH at  $37^\circ\text{C}$ . Aliquots of the acid-insoluble and the acid-soluble (pooled supernatants) fractions were taken for scintillation counting (LSC TRICARB 2500TR, Canberra Packard) using Pico-Fluor-15 (Canberra Packard, Meriden, Conn., USA). The viable cell number was determined in a Coulter counter (Coulter Electronics, Dunstable, UK) and by trypan blue staining (more than 94% viable cells). The measured radioactivity was standardised to the viable cell number and expressed as nmol/ $10^5$  cells.

**FDG uptake.** The uptake experiments were performed in glucose-free RPMI 1640 medium supplemented with glutamine and penicillin/streptomycin as described elsewhere [23, 24]. After 30 min of pre-incubation, 37 kBq 2-fluoro-2-deoxy-D- $^3\text{H}$ glucose (Amersham-Buchler; specific radioactivity 10.8 GBq/mmol; radioactive concentration 7.4 MBq/ml; radiochemical purity 99.3%) per millilitre of medium and cold FDG (0.1 mM final concentration) were added. After the cells had been incubated for 10 min, the medium was removed and the cells were washed twice with ice-cold PBS. The lysis was done on ice using ice-cold 0.6 M perchloric acid and a cell scraper. Thereafter, the lysates were neutralised with 1 M KOH and 0.5 M Tris/HCl (pH 7) and quantified by scintillation counting. The FDG uptake was also determined in the absence or presence of 10  $\mu\text{M}$  cytochalasin B or 1 mM deoxyglucose immediately after GCV treatment.

**3-O-Methylglucose uptake.** The uptake experiments were performed in glucose-free RPMI 1640 medium supplemented with glutamine and penicillin/streptomycin. After 30 min of pre-incubation, 185 kBq 3-O-methyl-D-[<sup>3</sup>H]glucose (Amersham-Buchler; specific radioactivity 92.5 GBq/mmol; radioactive concentration 37 MBq/ml, radiochemical purity 99.5%) per millilitre of medium and cold 3-O-methylglucose were added to a final concentration of 0.05 mM. After a 10-min incubation period, the medium was removed and the cells were washed twice with ice-cold PBS. The lysis was done on ice using 0.3 M NaOH/10% sodium dodecyl sulphate and a cell scraper. Scintillation counting was performed as described elsewhere [23, 24].

**Detection of apoptotic cells.** The measurement of apoptosis was done immediately and 24 h after the cells had been incubated with GCV for 24 h or had been treated with either 10 µM cytochalasin B or 1 mM deoxyglucose for 4 h as monotherapy. If the substances were used in combination for the treatment of the cells, either 10 µM cytochalasin B or 1 mM deoxyglucose was added to the GCV-containing medium for the last 4 h. Cells were seeded on collagen-coated glass cover slips in culture medium. After removal of the medium, DNA fragmentation was studied in 4% paraformaldehyde-fixed cells by the TUNEL technique, using a commercially available in situ cell death detection kit (Oncor, Heidelberg, Germany) as previously described [19, 21, 22]. Thereafter nuclei were counterstained with haematoxylin and the percentage of TUNEL-positive cells was quantified by the use of a light microscope in addition to computer-assisted morphometry. Furthermore, the experiments were done using unfixed cells and YOPRO-1 staining [25].

**Statistical analysis.** Statistical procedures were performed with the SIGMASTAT program (Jandel Scientific, Erkrath, Germany). Statistical significance was determined by the *t* test. A *P* value of <0.05 was considered statistically significant.

## Results

### Expression of GLUT1 and GLUT3 in HSVtk-expressing Morris hepatomas during GCV treatment

Data in respect of glucose transporter expression were available for five control tumours and five tumours from GCV-treated animals showing elevated FDG transport into the tumour [17]. The quantitation of GLUT1- or GLUT3-positive cells revealed an increased amount of both transporters in tumours with enhanced FDG transport (Fig. 1), although the  $K_1$  values for FDG transport into the tumour and the amount of GLUT1-positive cells were not correlated. However, a statistically significant difference was seen between untreated and treated tumours for GLUT1 ( $P=0.04$ ).

### TdR uptake in the acid-soluble and acid-insoluble fractions immediately and 24 h after therapy

To assess the effects of *HSVtk* gene therapy on DNA synthesis, TdR uptake was studied in the acid-insoluble

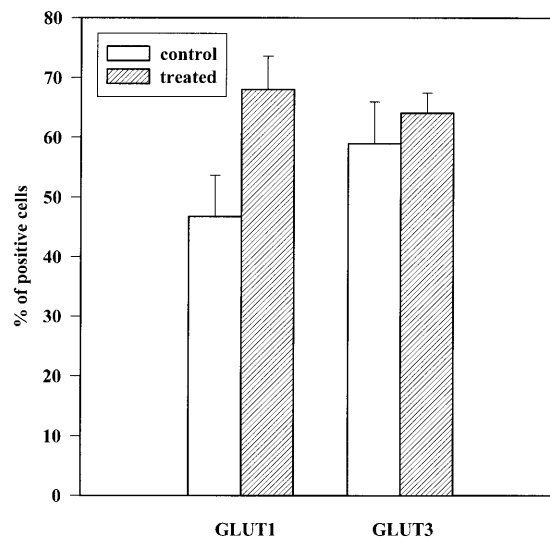
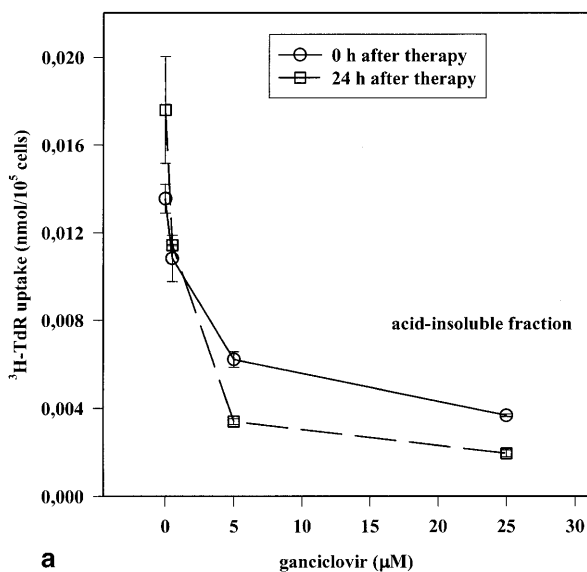


**Fig. 1.** Percentages of GLUT1- and GLUT3-positive cells in samples from control tumours and tumours after GCV treatment. Statistically significant differences were found for GLUT1 ( $P=0.04$ ). Mean values and standard error are shown ( $n=5$ )

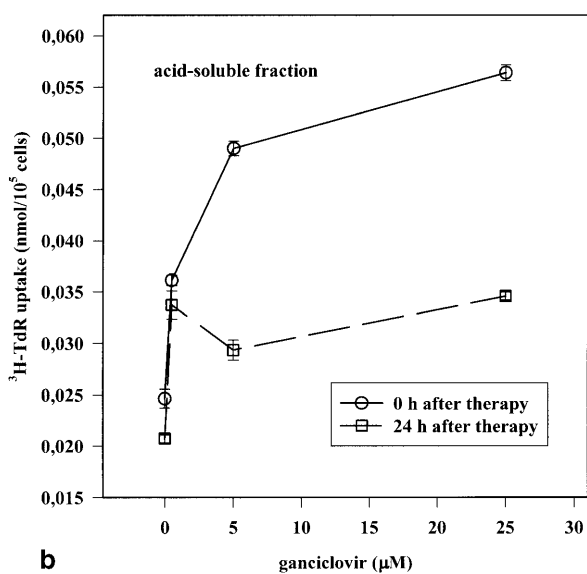
(representing nucleic acids and proteins) and the acid-soluble fraction (representing unbound radioactivity in acid-soluble molecules that are not in DNA and proteins) after perchloric acid extraction. In the acid-insoluble fraction, a dose-dependent decrease in thymidine uptake to 27% and 11% of the control value was found immediately and 24 h after therapy, respectively (Fig. 2a). However, for the acid-soluble fraction a dose-dependent increase to 229% of the control value was seen immediately after GCV therapy, whereas 24 h after the treatment the increase in TdR uptake in this fraction was lower (167% of control, Fig. 2b).

### Effect of increasing GCV concentrations on FDG and 3-O-methylglucose uptake immediately and 24 h after therapy

In vitro a combined uptake experiment was done with FDG, which is transported and phosphorylated, and 3-O-methylglucose, which shows no significant metabolism. Immediately after the *HSVtk*-expressing cells had been incubated for 24 h with increasing concentrations of GCV, FDG uptake was observed to be increased to 183% of that in untreated cells, whereas 24 h after the end of GCV exposure no significant differences were found between GCV-treated cells and the untreated cells (Fig. 3a). 3-O-Methylglucose uptake also increased instantly after therapy, to 186%, but, in contrast to the results for FDG, this increase persisted 24 h after the end of GCV incubation (Fig. 3b). Uptake measurements in the presence of cytochalasin B or deoxyglucose resulted in a 78% and 88% decrease in FDG uptake, respectively (Fig. 3c).

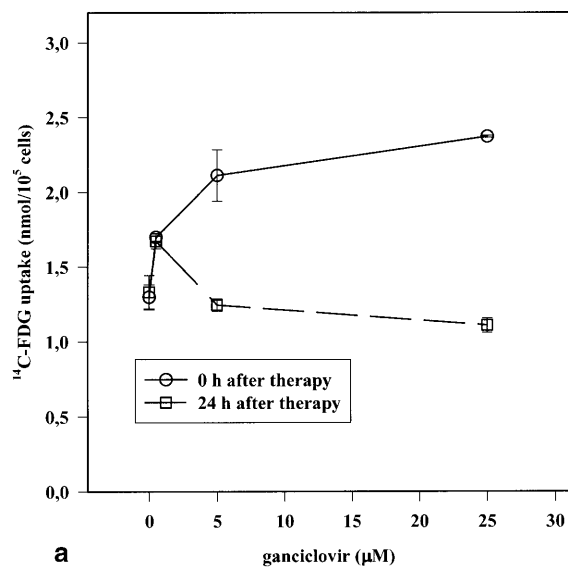


a

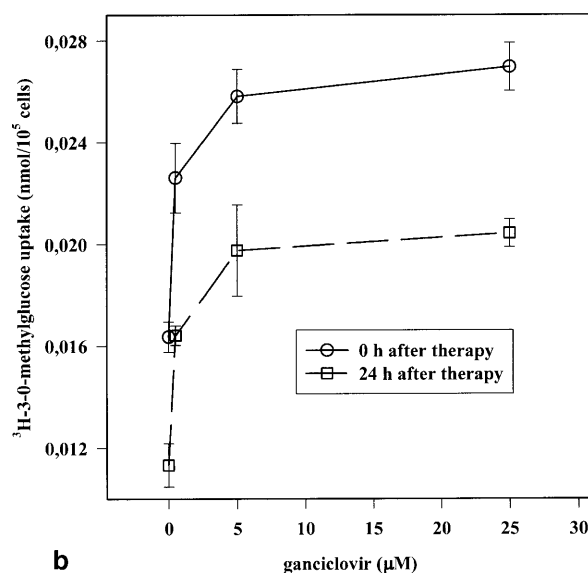


b

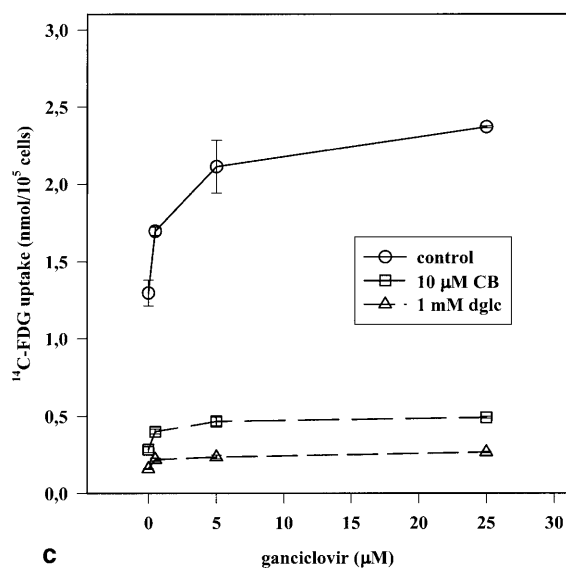
**Fig. 2.** Thymidine uptake (nmol/10<sup>5</sup> cells) in the acid-insoluble (a) and the acid-soluble (b) fraction of *HSVtk*-expressing Morris hepatoma cells immediately and 24 h after the end of treatment with 0, 0.5, 5 and 25 μM ganciclovir (GCV). A significant decrease in tracer uptake in the acid-insoluble fraction and an increase in the acid-soluble fraction were observed. Mean values and standard deviations are shown ( $n=3$ )



a



b



c

**Fig. 3.** FDG (a) and 3-*O*-methylglucose (b) uptake (nmol/10<sup>5</sup> cells) in *HSVtk*-expressing Morris hepatoma cells immediately and 24 h after the end of treatment with 0, 0.5, 5 and 25 μM ganciclovir (GCV). The presence of either 10 μM cytochalasin B (CB) or 1 mM deoxyglucose (*dglc*) caused a significant decrease in tracer uptake (c). Mean values and standard deviations are shown ( $n=3$ )

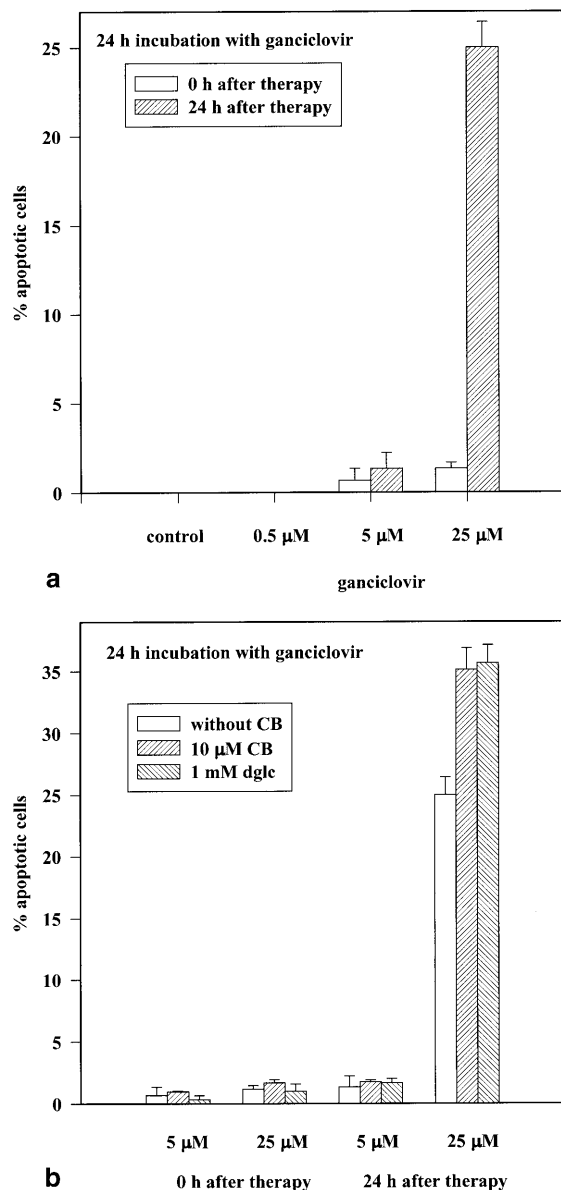


**Fig. 4.** **a** Percentage of apoptotic cells immediately and 24 h after the end of treatment with 0, 0.5, 5 and 25  $\mu\text{M}$  ganciclovir (GCV). The percentage of TUNEL-positive cells is shown. **b** Percentage of apoptotic cells immediately and 24 h after the end of treatment with 0, 0.5, 5 and 25  $\mu\text{M}$  ganciclovir with or without 10  $\mu\text{M}$  cytochalasin B (CB) or 1 mM deoxyglucose (dglc). Mean values and standard deviations are shown ( $n=3$ )

#### Effect of increasing GCV concentrations on percentage of apoptotic cells immediately and 24 h after therapy

The percentage of apoptotic cells was determined using the TUNEL assay but similar data were obtained by use of YOPRO-1 staining (data not shown). Immediately after the end of GCV incubation, only a few apoptotic cells were found. However, 24 h after the end of therapy a significant increase (20-fold) in the apoptotic cell fraction was obtained using 25  $\mu\text{M}$  GCV. Lower doses of GCV

revealed no significant induction of apoptosis (Fig. 4a). Incubation with 10  $\mu\text{M}$  cytochalasin B or 1 mM deoxyglucose enhanced the therapeutic effect of GCV treatment. Monotherapy with cytochalasin B and deoxyglucose had no effect on apoptosis (data not shown). However, the combination of one of these agents with GCV caused a significant increase in the apoptotic cell fraction for the highest dose ( $P=0.002$  for deoxyglucose and  $P=0.003$  for cytochalasin B) (Fig. 4b).

## Discussion

Gene therapy of hepatoma cells with the *HSVtk/GCV* suicide system induced a decrease in  $^3\text{H}$ -thymidine accumulation in the acid-insoluble fraction, indicating an inhibition of thymidine incorporation into the DNA (Fig. 2a). However, thymidine uptake in the acid-soluble fraction increased, with a tendency towards normalisation at 24 h after therapy (Fig. 2b). The phenomenon of a post-therapeutic increase in thymidine or its metabolites in the acid-soluble fraction was also observed in former studies after chemotherapy with gemcitabine [24, 26]. This effect has been explained by an increase in the activity of salvage pathway enzymes such as the host thymidine kinase during repair of cell damage. These changes represent the cellular reaction to stress events that may lead to programmed cell death. An imbalance of the dNTP pool has been reported to induce the apoptotic cascade [27]. This occurs after treatment of tumour cells with antineoplastic agents that inhibit DNA precursor synthesis and also after interleukin-3 (IL-3) withdrawal in IL-3-dependent cell lines [27, 28, 29, 30]. The influence of the dNTP pool and of thymidine kinase activity on the protection of cells against apoptosis has also been shown in cells after transfection with the *HSVtk* gene, which conferred resistance to damaging agents [31]. Therefore, the increase in thymidine uptake in the acid-soluble fraction seems to reflect cellular stress reactions such as enhanced thymidine phosphorylation dedicated to the prevention of cell death.

Furthermore, we were able to demonstrate an increase in FDG and 3-*O*-methylglucose uptake immediately after the end of treatment, indicating an enhancement of glucose transport and phosphorylation (Fig. 3). At 24 h after the end of treatment, the FDG uptake had normalised whereas the uptake of the transport tracer 3-*O*-methylglucose was still elevated. This is evidence for an uncoupling of glucose transport and glucose phosphorylation, which we previously observed in vivo [17]. Similar FDG-PET data were obtained after treatment of Morris hepatoma with gemcitabine, and these phenomena also occurred in human tumour xenografts after radiation therapy [24, 32]. In a study with three tumour models, the most radiosensitive tumour with the highest incidence of radiation-induced apoptosis displayed a 2.3-fold higher rate of [ $^{18}\text{F}$ ]FDG accumulation at 2 h follow-

ing irradiation compared with a non-irradiated group, and thereafter showed a plateau in the accumulation up to 6 h. However, the accumulation did not increase significantly in tumours with lower radiosensitivity and much less radiation-induced apoptosis [32]. In several studies these changes have been explained by a translocation of preformed glucose transport proteins from intracellular compartments to the plasma membrane, found to occur in treated tumour cells but also in non-malignant tissues as a transcription-independent early reaction to different cellular stresses [23, 24, 26, 33, 34, 35]. In our study, an immunohistochemical analysis of tumours treated with the *HSVtk/GCV* suicide system revealed an enhanced amount of GLUT1- and GLUT3-positive cells in tumours exhibiting increased FDG transport (the kinetic constant  $K_1$  for FDG transport into the tumour was  $0.06 \pm 0.02$  ml/min per gram for control tumours and  $0.19 \pm 0.02$  ml/min per gram for treated tumours [17]); the result was, however, statistically significant only for GLUT1 (Fig. 1). The fact that  $K_1$  was not correlated with GLUT1-positive cells may have been due to sampling variability and heterogeneity of the tumours. Furthermore,  $K_1$  is determined not only by GLUT1 but also by other GLUT isotypes. In this study we were also able to show GLUT3 expression in the tumours.

The fact that the glucose transport was elevated at lower doses of GCV, at which no apoptosis occurred, suggests that there exists a threshold level of cellular damage. Below this level apoptosis is compensated by cellular stress reactions consisting of stabilisation of the intracellular nucleoside triphosphate pool, enhancement of glucose transport or other mechanisms. If enhancement of glucose uptake represents one of the mechanisms for the protection of cells from programmed cell death, inhibition of glucose transport should enhance apoptosis. Consequently, we incubated cells with cytochalasin B, a fungal metabolite that binds to the inner part of the glucose transporter, for the last 4 h of GCV treatment. We found a decrease in FDG uptake in the presence of cytochalasin B as compared with the controls (Fig. 3c) and an increase in apoptosis at 24 h after the end of combination treatment with GCV and cytochalasin B (Fig. 4b), whereas monotherapy with CB was not sufficient to induce apoptosis (data not shown). However, since cytochalasin B is highly toxic and, therefore, not applicable in humans, we used deoxyglucose, which competes with glucose and FDG for transport and phosphorylation and can be applied in patients to enhance the outcome of suicide gene therapy. As a monotherapy with low concentration and short exposure time for the cells, no induction of apoptosis was seen (data not shown). However, when used in combination with GCV, deoxyglucose also caused a decrease in FDG uptake (Fig. 3c) as well as an increase in the percentage of apoptotic cells (Fig. 4b). Similar results have been obtained after treatment of Morris hepatoma with gemcitabine or after a combination of deoxyglucose or the mitochondrial li-

gand rhodamine-123 and tumour necrosis factor in U937 histiocytic lymphoma cells [24, 36].

In general, a combination of cytotoxic therapy with inhibitors of glucose metabolism may enhance the effects but also the side-effects due to stress reactions induced in the tumour and in normal tissues [37]. Consequently, combination with chemotherapeutic drugs may not result in therapeutic benefit for patients, although for some drugs normal tissues recover more quickly than the tumour [37, 38]. This may not be the case for gene therapy, because the tumour can be targeted selectively, for example by use of tissue-specific vectors. Therefore, future studies need to address possible synergistic effects of this combined therapy in vivo. For the planning of these combined treatment strategies, PET with [ $^{18}\text{F}$ ]FDG may be used to detect early reactions of the tumour to stress induced by gene therapy or chemotherapy, as has been found in a variety of tumour models [16, 17, 23, 24, 26, 35, 37].

*Acknowledgements.* We thank Ellen Bender for her help in performing this study. This study was supported by a grant from the Tumorzentrum Heidelberg/Mannheim.

## References

- Chen SH, Shine HD, Goodman JC, Grossman RG, Woo SLC. Gene therapy for brain tumors: regression of experimental gliomas by adenovirus-mediated gene transfer in vivo. *Proc Natl Acad Sci U S A* 1994; 91:3054–3057.
- Moolten FL, Wells JM. Curability of tumors bearing herpes thymidine kinase genes transferred by retroviral vectors. *J Natl Cancer Inst* 1990; 82:297–300.
- Caruso M, Panis Y, Gagandeep S, Houssin D, Salzman JL, Klatzman D. Regression of established macroscopic liver metastases after in situ transduction of a suicide gene. *Proc Natl Acad Sci U S A* 1993; 90:7024–7028.
- Oldfield EH, Ram Z, Culver KW, Blaese RM, DeVroom HL, Anderson WF. Gene therapy for the treatment of brain tumors using intra-tumoral transduction with the thymidine kinase gene and intravenous ganciclovir. *Hum Gene Ther* 1993; 1: 39–69.
- Culver KW, Ram Z, Walbridge S, et al. In vivo gene transfer with retroviral vector-producer cells for treatment of experimental brain tumors. *Science* 1992; 256:1550–1552.
- Ring CJA, Blouin P, Martin LA, Hurst HC, Lemoine NR. Use of transcriptional regulatory elements of the *MUC1* and *ERBB2* genes to drive tumor-selective expression of a prodrug activating enzyme. *Gene Ther* 1997; 4:1045–1052.
- Keller PM, Fyfe JA, Beauchamp L, et al. Enzymatic phosphorylation of acyclic nucleoside analogs and correlations with antiherpetic activities. *Biochem Pharmacol* 1981; 30: 3071–3077.
- Bi WL, Parysk LM, Warnick R, Stambrook PJ. In vitro evidence that metabolic cooperation is responsible for the bystander effect observed with *HSV-tk* retroviral gene therapy. *Hum Gene Ther* 1993; 4:725–731.
- Hamel W, Magnelli L, Chiarugi VP, Israel MA. Herpes simplex virus thymidine kinase/ganciclovir-mediated apoptotic death of bystander cells. *Cancer Res* 1996; 56:2697–2702.

10. Ishii-Morita H, Agbaria R, Mullen CA, et al. Mechanism of bystander effect killing in the herpes simplex thymidine kinase gene therapy model of cancer treatment. *Gene Ther* 1997; 4:244–251.
11. Samejima Y, Meruelo D. 'Bystander killing' induces apoptosis and is inhibited by forskolin. *Gene Ther* 1995; 2:50–58.
12. Beltinger C, Fulda S, Kammertoens T, et al. Herpes simplex thymidine kinase/ganciclovir-induced apoptosis involves ligand-independent death receptor aggregation and activation of caspase. *Proc Natl Acad Sci U S A* 1999; 96:8699–8704.
13. Eguchi Y, Shimizu S, Tsujimoto Y. Intracellular ATP levels determine cell death fate by apoptosis or necrosis. *Cancer Res* 1997; 57:1835–1840.
14. Leist M, Single B, Castoldi AF, Kühnle S, Nicotera P. Intracellular adenosine triphosphate (ATP) concentration: a switch in the decision between apoptosis and necrosis. *J Exp Med* 1997; 185:1481–1486.
15. Garland JM, Halestrap A. Energy metabolism during apoptosis. *J Biol Chem* 1997; 272:4680–4688.
16. Haberkorn U, Altmann A, Morr I, Germann C, Oberdorfer F, van Kaick G. Multi tracer studies during gene therapy of hepatoma cells with HSV thymidine kinase and ganciclovir. *J Nucl Med* 1997; 38:1048–1054.
17. Haberkorn U, Bellemann ME, Gerlach L, et al. Uncoupling of 2-fluoro-2-deoxyglucose transport and phosphorylation in rat hepatoma during gene therapy with HSV thymidine kinase. *Gene Ther* 1998; 5:880–887.
18. Haberkorn U, Altmann A, Morr I, et al. Gene therapy with herpes simplex virus thymidine kinase in hepatoma cells: uptake of specific substrates. *J Nucl Med* 1997; 38:287–294.
19. Kinscherf R, Deigner HP, Usinger C, et al. Induction of manganese superoxide dismutase by oxidized-LDL – its relevance in atherosclerosis of humans and heritable hyperlipidemic rabbits. *FASEB J* 1997; 11:1317–1328.
20. Kinscherf R, Claus R, Wagner M, Gehrke C, Kamencic H, Hou D, Chen M, Nauen O, Schmiedt W, Kovacs G, Pill J, Metz J, Deigner HP. Apoptosis caused by oxidized-LDL is manganese superoxide dismutase and p53-dependent. *FASEB J* 1998; 12:461–467.
21. Kollum M, Kaiser S, Kinscherf R, Metz J, Kübler W, Hehrlein C. Apoptosis after stent implantation compared with balloon angioplasty in rabbits. The role of macrophages. *Arterioscler Thromb Vasc Res* 1997; 17:2383–2388.
22. Kinscherf R, Wagner M, Kamencic H, et al. Characterization of apoptotic macrophages in atheromatous tissue of humans and heritable hyperlipidemic rabbits. *Atherosclerosis* 1999; 144:33–39.
23. Haberkorn U, Morr I, Oberdorfer F, et al. FDG uptake in vitro: aspects of method and effects of treatment with gemcitabine. *J Nucl Med* 1994; 35:1842–1850.
24. Haberkorn U, Bellemann ME, Brix G, et al. Apoptosis and changes in glucose metabolism after treatment of Morris hepatoma with gemcitabine. *Eur J Nucl Med* 2001; 28:418–425.
25. Idziorek T, Estaquier J, De Bels F, Ameisen JC. YOPRO-1 permits cytofluorometric analysis of programmed cell death (apoptosis) without interfering with cell viability. *J Immunol Methods* 1995; 185:249–258.
26. Haberkorn U, Bellemann ME, Altmann A, et al. F-18-fluoro-2-deoxyglucose uptake in rat prostate adenocarcinoma during chemotherapy with 2',2'-difluoro-2'-deoxycytidine. *J Nucl Med* 1997; 38:1215–1221.
27. Oliver FJ, Collins MK, Lopez-Rivas A. Regulation of the salvage pathway of deoxynucleotides synthesis in apoptosis induced by growth factor deprivation. *Biochem J* 1996; 316:421–425.
28. Oliver F, Marvel J, Collins MKL, Lopez-Rivas A. *Bcl-2* oncogene protects a bone marrow-derived pre-B-cell line from 5'-fluor,2'-deoxyuridine-induced apoptosis. *Biochem Biophys Res Commun* 1993; 194:126–132.
29. Miyashita T, Reed JC. *bcl-2* gene transfer increases relative resistance of S49.1 and WEHI7.2 lymphoid cells to cell death and DNA fragmentation induced by glucocorticoids and multiple chemotherapeutic drugs. *Cancer Res* 1992; 52:5407–5411.
30. Kizaki H, Shimada H, Osaka F, Sakurada E. Adenosine, deoxyadenosine and deoxyguanosine induce DNA cleavage in mouse thymocytes. *J Immunol* 1988; 141:1652–1659.
31. Oliver FJ, Collins MKL, Lopez-Rivas A. Overexpression of a heterologous thymidine kinase delays apoptosis induced by factor deprivation and inhibitors of deoxynucleotide metabolism. *J Biol Chem* 1997; 272:10624–10630.
32. Furuta M, Hasegawa M, Hayakawa K, et al. Rapid rise in FDG uptake in an irradiated human tumor xenograft. *Eur J Nucl Med* 1997; 24:435–438.
33. Widnell CC, Baldwin SA, Davies A, Martin S, Pasternak CA. Cellular stress induces a redistribution of the glucose transporter. *FASEB J* 1990; 4:1634–1637.
34. Clancy BM, Czech MP. Hexose transport stimulation and membrane redistribution of glucose transporter isoforms in response to cholera toxin, dibutyryl cyclic AMP, and insulin in 3T3 adipocytes. *J Biol Chem* 1990; 265:12434–12443.
35. Smith TAD, Maisey NR, Titley JC, Jackson LE, Leach MO, Ronen SM. Treatment of SW620 cells with tomudex and oxiplatin induces changes in 2-deoxy-D-glucose incorporation associated with modifications in glucose transport. *J Nucl Med* 2000; 41:1752–1759.
36. Halicka HD, Ardelt B, Li X, Melamed MM, Darzynkiewicz Z. 2-Deoxy-D-glucose enhances sensitivity of human histiocytic lymphoma U937 cells to apoptosis induced by tumor necrosis factor. *Cancer Res* 1995; 55:444–449.
37. Haberkorn U, Reinhardt M, Berger MR, et al. Metabolic design of combination therapy: use of enhanced fluorodeoxyglucose uptake caused by chemotherapy. *J Nucl Med* 1992; 33:1981–1987.
38. Milas L, Fujii T, Hunter N, et al. Enhancement of tumor radioresponse in vivo by gemcitabine. *Cancer Res* 1999; 59:107–114.